Science of the Total Environment 563–564 (2016) 329–339

Contents lists available at ScienceDirect

Science of the Total Environment

journal homepage: www.elsevier.com/locate/scitotenv

Composition and fate of mine- and smelter-derived particles in soils of humid subtropical and hot semi-arid areas

Vojtěch Ettler [a,*], Zdenek Johan [b,1], Bohdan Kříbek [c], František Veselovský [c], Martin Mihaljevič [a], Aleš Vaněk [d], Vít Penížek [d], Vladimír Majer [c], Ondra Sracek [e], Ben Mapani [f], Fred Kamona [f], Imasiku Nyambe [g]

[a] Institute of Geochemistry, Mineralogy and Mineral Resources, Faculty of Science, Charles University in Prague, Albertov 6, 128 43 Praha 2, Czech Republic
[b] BRGM, Avenue Claude Guillemin, 45082 Orléans Cedex 2, France
[c] Czech Geological Survey, Geologická 6, 152 00 Praha 5, Czech Republic
[d] Department of Soil Science and Soil Protection, Faculty of Agrobiology, Food and Natural Resources, Czech University of Life Sciences Prague, Kamýcká 129, 165 21 Praha 6, Czech Republic
[e] Department of Geology, Faculty of Science, Palacký University in Olomouc, 17. listopadu 12, 771 46 Olomouc, Czech Republic
[f] Department of Geology, Faculty of Science, University of Namibia, Private Bag 13301, Windhoek, Namibia
[g] University of Zambia, School of Mines, P. O. Box 32 379, Lusaka, Zambia

HIGHLIGHTS

- Mining- and smelter-derived particles identified in subtropical and semi-arid soils
- Sulphides, oxides, and metal-bearing arsenates most frequently encountered
- Soluble sulphates and arsenolite from primary smelter dusts not detected in soils
- Higher metal availability and greater weathering of particles in subtropical soils
- Complex Ca–Cu–Pb arsenates efficiently control mobility of metal(loids).

GRAPHICAL ABSTRACT

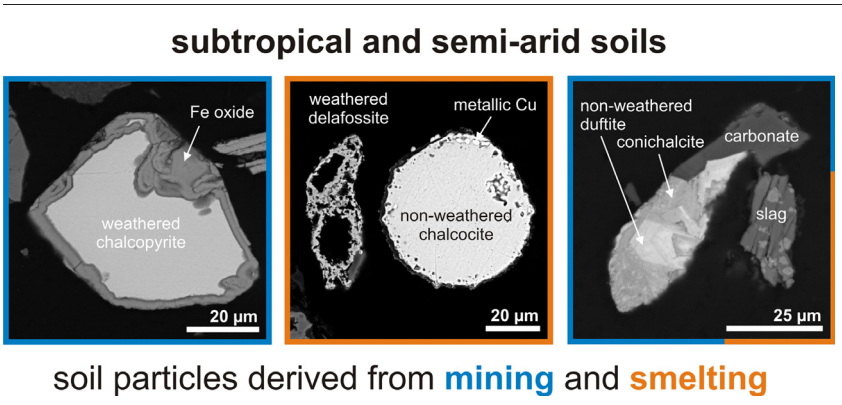

ARTICLE INFO

Article history:
Received 24 February 2016
Received in revised form 13 April 2016
Accepted 18 April 2016
Available online xxxx

Editor: F.M. Tack

Keywords:
Soil
Heavy mineral fraction
Mining
Smelting

ABSTRACT

We studied the heavy mineral fraction, separated from mining- and smelter-affected topsoils, from both a humid subtropical area (Mufulira, Zambian Copperbelt) and a hot semi-arid area (Tsumeb, Namibia). High concentrations of metal(loid)s were detected in the studied soils: up to 1450 mg As kg^{-1}, 8980 mg Cu kg^{-1}, 4640 mg Pb kg^{-1}, 2620 mg Zn kg^{-1}. A combination of X-ray diffraction analysis (XRD), scanning electron microscopy (SEM/EDS), and electron probe microanalysis (EPMA) helped to identify the phases forming individual metal(loid)-bearing particles. Whereas spherical particles originate from the smelting and flue gas cleaning processes, angular particles have either geogenic origins or they are windblown from the mining operations and mine waste disposal sites. Sulphides from ores and mine tailings often exhibit weathering rims in contrast to smelter-derived high-temperature sulphides (chalcocite [Cu_2S], digenite [Cu_9S_5], covellite [CuS], non-stoichiometric quenched Cu–Fe–S phases). Soils from humid subtropical areas exhibit higher available concentrations of metal(loids), and higher frequencies of weathering features (especially for copper-bearing oxides such as delafossite [$Cu^{1+}Fe^{3+}O_2$]) are observed. In contrast, metal(loid)s are efficiently retained in semi-arid soils, where a high proportion of non-weathered smelter slag

* Corresponding author.
E-mail address: ettler@natur.cuni.cz (V. Ettler).
[1] Deceased February 13, 2016.

http://dx.doi.org/10.1016/j.scitotenv.2016.04.133

Mineralogy
Weathering

particles and low-solubility Ca–Cu–Pb arsenates occur. Our results indicate that compared to semi-arid areas (where inorganic contaminants were rather immobile in soils despite their high concentrations) a higher potential risk exists for agriculture in mine- and smelter-affected humid subtropical areas (where metal(loid) contaminants can be highly available for the uptake by crops).

1. Introduction

Emissions from mines and non-ferrous metal smelters are responsible for the contamination of various environmental compartments in the vicinity of such industrial operations (Csavina et al., 2012, 2014; Shukurov et al., 2014). Soils represent major sinks for emitted metal(loid)-bearing particulates (aerosol size; <10 μm), and also for larger particles. As a result, high levels of inorganic contaminants have been observed, especially in the surficial soil layers around mines and smelters (Ettler (2016) and references therein). The prevailing wind direction and the size of particulates/particles are key parameters affecting the spatial distribution of smelter- and mine-related contamination, with higher rates of dispersion in dry and semi-arid areas (e.g., Csavina et al., 2011, 2012; Ettler, 2016; Kříbek et al., 2014a, 2014b, 2016; Mihaljevič et al., 2015). Thus, in terms of spatial distribution, the contamination hotspots in soils are generally elongated, and exhibit their highest metal(loid) concentrations downwind from the mines and smelters (Ettler et al., 2011, 2014a; Ettler, 2016; Kříbek et al., 2010, 2016). Csavina et al. (2011, 2014) reported that ultrafine smelter-derived aerosols (<0.5 μm in size) are particularly rich in contaminants, and they may travel over long distances. Moreover, variability in dry and wet deposition can also affect the distribution of particulates/particles near smelters. Schindler et al. (2012) and Caplette et al. (2015) studied alteration crusts on rocks near several Canadian smelters. They found that an increase in metal(loid) concentrations and the greater occurrence of metal(loid)-bearing particulates embedded in these black rock coatings 2 km from the smelter stack may be attributed to a "shadow effect", which results from precipitation events and the gravitational settling of larger particulates causing their deposition. It was argued that especially the smaller metal-sulphate aerosols might be washed out from the atmosphere during precipitation events, and thus their spatial influence might be limited during wet periods (Schindler et al., 2012; Sorooshian et al., 2012).

A number of studies have been devoted to mineralogical investigations of particulates (<10 μm) as well as larger particles, collected near mining and smelting operations: encapsulated in alteration layers on rocks (Caplette et al., 2015; Mantha et al., 2012; Schindler et al., 2012), trapped in soils from temperate areas (Adamo et al., 1996; Cabala and Teper, 2007; Henderson et al., 1998; Knight and Henderson, 2006; Lanteigne et al., 2012, 2014), or in snowpack (Gregurek et al., 1998, 1999). Interestingly, except for a few studies (e.g., Chopin and Alloway, 2007; Ettler et al., 2014a, 2014b; Gutiérrez-Ruiz et al., 2012), the mineralogical and chemical compositions of mining- and smelter-derived particulates and particles in soils of subtropical and tropical climatic zones have not yet been studied.

The aim of this study was to provide insights into the variability of chemical and mineralogical compositions of particulates/particles emitted from non-ferrous metal mining and smelting operations and deposited into the soils of humid subtropical and dry semi-arid areas in southern Africa. We also focused on the assessments and comparisons of their weathering features, as well as their potential role in the release and fate of metal(loid) contaminants into these soil systems.

2. Materials and methods

2.1. Study areas and soil sampling

The studied soils were sampled in two mining and smelting areas (Fig. 1): (i) Mufulira in the Zambian Copperbelt (mean annual precipitation 1270 mm, mean annual temperature 19.7 °C, humid subtropical climate [Cwa] according to the Köppen climate classification); (ii) Tsumeb in northern Namibia (mean annual precipitation 550 mm, mean annual temperature 22 °C, hot semi-arid climate [BSh] according to the Köppen climate classification) (climate-data.org). In both regions, there is a distinct rainy season (November–April) and a dry season (May–October); the strongest winds occur during the dry seasons, these being south-easterly (Fig. 1).

Mufulira is located in a Cu—Co mining and smelting area, where ore extraction and processing activities date back to the 1930s. The ore in the Mufulira deposit is characterised by a stratabound disseminated mineralisation in footwall arkoses and conglomerates; the main ore minerals being bornite (Cu_5FeS_4), followed by chalcocite (Cu_2S), chalcopyrite ($CuFeS_2$), covellite (CuS), and cobaltiferous pyrite. The Mufulira copper smelter was initially commissioned in 1937, and was equipped with reverbatory furnaces and later with electric furnaces; in 2006, the smelting process was upgraded, when Isasmelt technology was commissioned (more information is given in Kříbek et al. (2010); Schlesinger et al. (2011); and Vítková et al. (2010)). The offgas is first cooled in heat recovery boilers, and afterwards electrostatic precipitators (ESP) are used for dust removal.

The Tsumeb deposit belongs to the northern Namibian sulfidic metallogenic province, which is part of the Otavi group formed of limestones and dolomites of Neoproterozoic age. This deposit is predominantly of a Pb–Cu–Zn type and contains a large variety of metal(loid)-bearing ore minerals, which also exhibited economic concentrations of Ag, Cd, Ge, and As. The deposit was mined in large open pits and several shafts from the beginning of the 20th century until 2006. The smelter at Tsumeb began operations in 1907, when blast furnaces were constructed to process the local Pb—Cu ores. In 1963, new smelters were constructed, consisting of a Cu smelter with a reverbatory furnace and a Pb smelter with a shaft furnace. In the 1980′s, a slag mill was constructed for the processing of old Cu reverbatory slags, in which Pb and Cu were subsequently separated and granulated slags were produced. Currently, the Pb smelter is being dismantled, but the Cu smelter equipped with Ausmelt and reverbatory furnaces is still in operation, and now processes Cu concentrates from other localities (mainly from the Chelopech mine in Bulgaria). The offgas from the furnaces and converters is cooled in heat recovery boilers, and the dust is subsequently removed in baghouse facilities. The Tsumeb smelter is now one of the few in the world producing Cu from As-containing ores, with production of As_2O_3 as an intermediate product (more information about the mining and smelting activities is given in Bowell (2014); Ettler et al. (2009); Mihaljevič et al. (2015); Schlesinger et al. (2011), and at the company's website www.dundeeprecious.com).

The most polluted topsoils from profiles having been sampled during previous screening research in the Mufulira and Tsumeb areas (Ettler et al., 2014a; Mihaljevič et al., 2015; Podolský et al., 2015) were selected for this study. Soils from wooded (predominantly with miombo trees [*Brachystegia*, *Julbernardia*, and *Isoberlinia* spp.]) and grassland plots were sampled at three locations in the vicinity of Mufulira: (i) 3.6 km downwind from the Cu smelter, 2.5 km downwind from a mine tailing site; (ii) 8 km downwind from the Cu smelter, 5.5 km downwind from a mine tailing site; (iii) reference soils 25 km upwind from the Cu smelter and mine tailing sites (Fig. 1 and Table 1). Two soils were collected 1 km downwind from the Cu—Pb smelters and a few hundred meters from the tailing disposal sites in Tsumeb, where a mix of flotation mine wastes and slag dust are

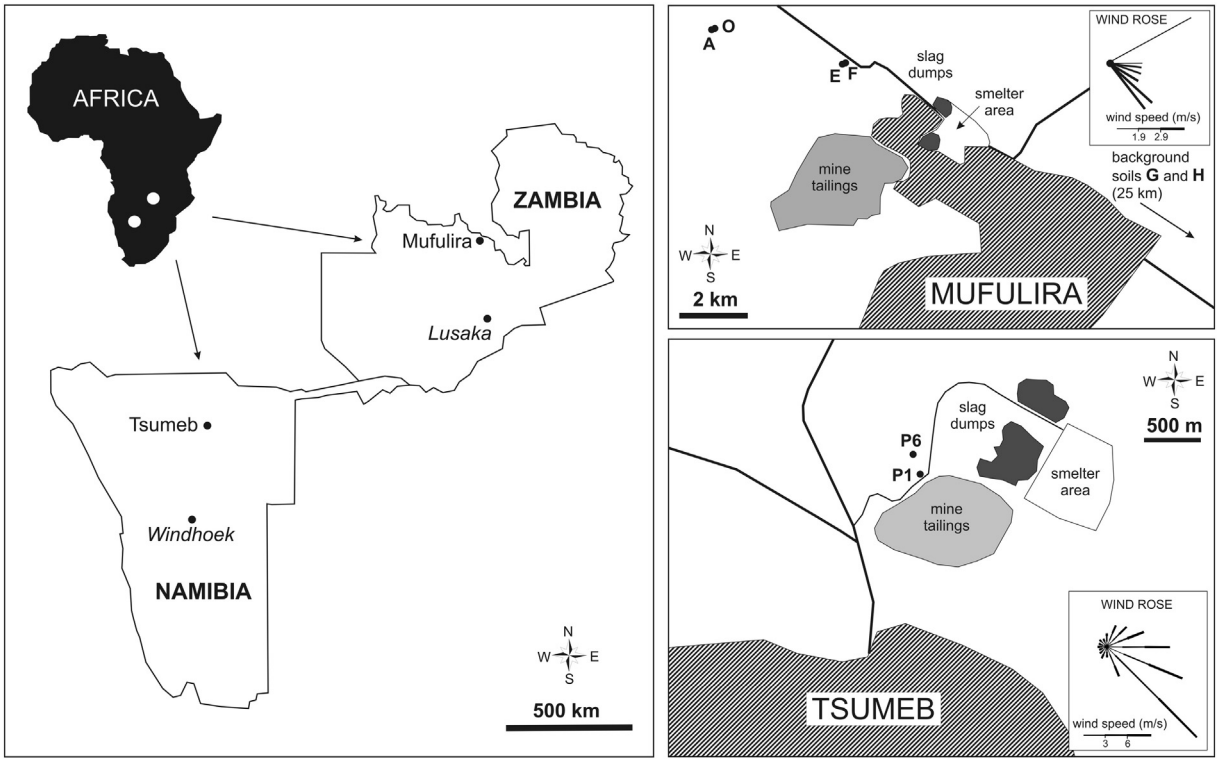

Fig. 1. Locations of the soil sampling sites near Mufulira, Zambian Copperbelt (a humid subtropical area); and Tsumeb, Namibia (a semi-arid area).

dumped. The soils in Tsumeb developed under open forest (predominated by marula trees [*Sclerocarya birrea*] and acacia trees/shrubs [*Acacia* spp.]) (Fig. 1 and Table 1).

The soil profiles were described according to the World Reference Base for Soil Resources (IUSS Working Group WRB, 2014). The soil samples were then stored in clean polyethylene (PE) bags and air-dried to a constant weight immediately upon return to the field laboratory. All of the soil samples were sieved through clean 2 mm stainless steel sieves (Retsch, Germany).

2.2. Soil properties determination and analysis

The soil colour was determined on moist samples using Munsell soil colour chart tables (Table 1). The soil pH was measured by a Schott

Table 1
Description and properties of the studied soils.

Sample/code	Depth	Distance to pollution source	Soil type and description	Munsell	pH	C_{org}/C_{inorg}	S_{tot} mg	CEC
Units	cm	km		colour	std units	g kg^{-1}	kg^{-1}	$cmol^{+}$ kg^{-1}
Subtropical soils[a]								
F1	0–1	3.6 (Cu smelter), 2.5 (tailings)	Haplic Ferralsol Eutric, grassland	7.5YR/3/1	5.46	53.7/<0.1	1250	5.89
E1	0–1	3.6 (Cu smelter), 2.5 (tailings)	Haplic Ferralsol Eutric, forest	10YR/4/1	5.39	98.5/<0.1	1190	15.1
A1	0–1	8 (Cu smelter), 5.5 (tailings)	Haplic Plinthosol Eutric, grassland	10YR/2/2	5.34	90.1/<0.1	1120	4.35
O1	0–1	8 (Cu smelter), 5.5 (tailings)	Haplic Ferralsol Xanthic, forest	7.5YR/3/1	6.85	57.3/<0.1	892	8.44
G1	0–1	25 (Cu smelter, tailings)	Stagnic Plinthosol Eutric, grassland, reference	7.5YR/4/1	6.55	31.8/<0.1	341	8.98
H1	0–1	25 (Cu smelter, tailings)	Haplic Ferralsol Dystric, forest, reference	5YR/5/1	5.10	21.3/<0.1	135	3.75
Semi-arid soils[b]								
P1	0–10	1 (Cu–Pb smelter), 0.1 (tailings)	Haplic Regosol, open forest	7.5YR/6/3	7.87	8.70/<0.1	411	9.50
P6	1-0[c]	1 (Cu–Pb smelter), 0.3 (tailings)	Spolic Technosol Calcaric Arenic, forest	7.5YR/3/3	6.73	241/19.8	4070	94.5

Sample/code	Cu	Co	Pb	Zn	Cd	As	Sb	V	Mineralogy of heavy fraction (XRD)[e]	Particles[f]	Me-particles[g]
Units	mg kg^{-1}	mg kg^{-1}	mg kg^{-1}	mg kg^{-1}	mg kg^{-1}	mg kg^{-1}	mg kg^{-1}	mg kg^{-1}			
F1	8980[d]	45.8	41.6	63.2	<2.5	5.10	<2.5	35.0	Tur, Zrn, Hem, Mi, Rt/Ant, Qz, Ccp, Bir	223	137
E1	2830	21.0	21.3	64.8	<2.5	6.31	<2.5	55.3	Tur, Gth, Hem, Zrn, Qz, Rt/Ant, Mi, Bir	16	3
A1	5480	25.2	39.1	83.3	<2.5	5.89	<2.5	58.3	Mag, Hem, Qz	1	0
O1	3320	23.5	17.9	50.8	<2.5	<5	<2.5	21.6	Tur, Rt, Hem, Zrn, Ilm, Cal	16	15
G1	37.4	2.70	<2.5	25.1	<2.5	<5	<2.5	24.6	Tur, Rt, Qz, Zrn, Ilm, Mi	2	0
H1	36.6	2.72	4.34	15.5	<2.5	<5	<2.5	20.9	Tur, Mi, Qz, Rt, Hem, Ilm, Zrn	5	2
P1	347	5.44	397	275	6.73	91.8	6.94	33.8	Qz, Rt, Ves, Hem, Dol, Zrn, Mag	66	40
P6	4470	13.6	4640	2620	96.7	1450	95.7	41.1	Dol, Ves, Con, Py, Fa, Hem, Duf, Qz, Rt, Gn	92	62

[a] Cu–Co mining/smelting, Mufulira, Copperbelt, Zambia, [b] Cu–Pb–Zn mining/smelting, Tsumeb, Namibia, [c] litter + humus, [d] mean values ($n = 2$) [e] Abbreviations of minerals: Ap — apatite ($Ca_5(PO_4)_3(OH,F,Cl)$); Bir — birnessite (MnO_2); Cal — calcite ($CaCO_3$); Ccp — chalcopyrite ($CuFeS_2$); Con — conichalcite ($CaCu(AsO_4)(OH)$); Duf — duftite ($PbCu(AsO_4)(OH)$); Fa — fayalite (Fe_2SiO_4); Gn — galena (PbS); Gth — goethite (FeOOH); Hem — haematite (Fe_2O_3); Ilm — ilmenite ($FeTiO_3$); Mag — magnetite (Fe_3O_4); Qz — quartz (SiO_2); Rt — rutile/Ant — anatase (TiO_2); Mi — mica (variable composition); Tur — tourmaline (mainly schorl: $NaFe_3Al_6Si_6O_{18}(BO_3)_3(OH)_4$); Ves — vesuvianite ($Ca_{10}(Mg,Fe)_2Al_4(SiO_4)_5(Si_2O_7)_2(OH,F)_4$); Zrn — zircon ($ZrSiO_4$). [f] number of particles analysed by SEM/EDS, [g] number of metal(loid)-bearing particles analysed by SEM/EDS.

Handylab pH meter equipped with a Schott BlueLine 28 pH electrode (Schott, Germany), in a 1:5 (w/v) soil-deionised water suspension after 1-h agitation (Pansu and Gautheyrou, 2006). The cation exchange capacity (CEC) was determined as the sum of the basic cations and Al extracted with 0.1 M $BaCl_2$ solution (Pansu and Gautheyrou, 2006). The basic cations and Al in the extracts were determined by flame atomic absorption spectrometry (FAAS; Varian SpectrAA 280 FS, Australia). Particle size distributions in the soil samples (fractions of clay, silt, and sand) were obtained by the hydrometer method (Gee and Or, 2002). The aliquot part of the soil under-sieve fraction was ground to analytical fineness in an agate ball mill (Fritsch, Germany) and used for determination of the total concentrations of major and trace elements in the soils, following digestion with HF and $HClO_4$. A weighed amount (0.2 g) of ground sample was dissolved in 10 ml of HF (49% v/v) and 0.5 ml of $HClO_4$ (70% v/v). The procedure was repeated with 5 ml HF (49% v/v) and 0.5 ml $HClO_4$ (70% v/v). Following evaporation, the sample was dissolved in 2 ml HNO_3, transferred into a 100 ml volumetric flask, diluted, and measured for total concentrations of As, Cd, Co, Cu, Pb, Sb, V, and Zn (being the main contaminants) either by inductively coupled plasma optical emission spectrometry (ICP-OES; ThermoScientific iCAP 6500, Germany) or by quadrupole-based inductively coupled plasma mass spectrometry (ICP-MS; ThermoScientific Xseries^{II}, Germany). The content of total sulphur (S_{tot}), total carbon (C_{tot}), and total inorganic carbon (C_{inorg}) was determined using a combination of ELTRA CS 530 and ELTRA CS 500 TIC analysers (combustion with infrared detection analyser; ELTRA, Germany). Total organic carbon (C_{org}) was calculated as C_{tot} - C_{inorg}.

The "labile" (available) contaminant fractions in the soils were determined by a 1 h extraction with 0.05 mol l^{-1} ethylendiammintetraacetic acid (EDTA) according to the methodology described by Quevauviller (1998). The extractions were conducted in duplicate. The extracts were filtered to 0.45 μm (Millipore® membrane filters), diluted to 2% (v/v) HNO_3, and analysed by ICP-OES or ICP-MS. We are aware that this standardised methodology was originally designed for metals; however, for the sake of simplicity, we also used the same extraction method for metalloids.

The quality of the analytical procedure for soil digestion/analysis was controlled using reference materials SRM 2710 (NIST, USA, Montana Soil, highly elevated trace element concentrations) and SRM 2711a (NIST, USA, Montana II Soil, moderately elevated trace element concentrations). The accuracy of the ICP measurement of metal(loid)s in leachates and extracts was controlled by parallel analysis of the reference material SRM 1640 (NIST, USA, Trace elements in natural water). The quality control/quality assurance (QC/QA) results of the measurements are reported in Table S1 in the Supplementary Material, and indicate good agreements between the measured and certified values (better than 9% relative standard deviation, RSD).

2.3. Mineralogical investigation of metal(loid)-bearing particles

The heavy mineral fraction was separated from bulk soil samples. For the separation, we used 1,1,2,2-tetrabromethane (density 2.96 g cm^{-3}) in a centrifuge (Janetzki S70D, Germany) at 1800 rpm for 30 min. The phase composition of the samples was assessed by X-ray diffraction analysis (XRD) using a PANalytical X'Pert Pro diffractometer (PANalytical, the Netherlands) with a X'Celerator detector, CuKα radiation (λ = 1.5418 Å) at 40 kV and 30 mA, over the range 2–80° 2theta, with a step of 0.02°, and a counting time of 150 s per step. For the analysis of the XRD patterns, X'Pert HighScore Plus 3.0 software coupled to the Crystallography Open Database (COD) (Gražulis et al., 2012) was used.

Polished sections were prepared from the heavy mineral fraction of the soils; the polishing has been performed in alcohol to limit potential dissolution of individual phases in water. Specimens were examined under a Leica DM LP (Leica, Germany) polarizing microscope and subsequently studied by a scanning electron microscope (SEM; TESCAN VEGA3XM, Czech Republic) equipped with an energy dispersion spectrometer (EDS; Quantax 200 X-Flash 5010, Bruker, Germany). Preliminary quantitative microanalyses were performed using a TESCAN VEGA SEM (TESCAN, Czech Republic) equipped with an Oxford Link X-Max 50 EDS (Oxford Instruments, UK) calibrated against the SPI set of standards (SPI supplies, USA), and operating at 15 kV with a beam current of 1.5 nA. >800 EDS analyses were performed using SEM. The quantitative analyses of representative phases were measured by electron microprobe (EPMA; Cameca SX-100, France). Operating conditions for measurement of the sulphides were the following: accelerating voltage 20 keV, beam current 7 nA, standards (analytical lines in parentheses): Ag metal (AgLα), stibnite (SbLα), galena (PbMα), GaAs (AsLß), marcasite (FeKα), Cu metal (CuKα), Zn metal (ZnKα), sphalerite (SKα), pentlandite (NiKα), Co metal (CoKα). Counting time was between 10 and 30 s on peaks and background, and the spot size was 1 μm. Operating conditions for measurement of oxygen-bearing phases (silicates, oxides, arsenates, etc.) were the following: accelerating voltage 15 keV, beam current 10 nA, standards (analytical lines in parentheses): diopside (MgKα, CaKα), quartz (SiKα), jadeite (AlKα), apatite (PKα), barite (SKα), rutile (TiKα), spinel (MnKα), haematite (FeKα), GaAs (AsLα), willemite (ZnLα), Pb metal (PbMα), cuprite (CuLα), Sb_2Te_3 (SbLα), V_2O_5 (VKα), CdTe (CdLα), Ni metal (NiKα), Co metal (CoKα). Counting time was between 10 and 60 s on peaks and background, and the spot size was 1 μm, with an enlarged beam size for the measurements of the glass phase and arsenates and/or arsenites unstable under the beam. In total, >110 spot analyses were performed using EPMA.

3. Results and discussion

3.1. Soil properties

A detailed description and the properties of the soils studied are reported in Table 1. The pH of soils from the Zambian Copperbelt ranged from slightly acidic to near-neutral (5.10–6.85), while topsoils from Namibia were near-neutral to alkaline (6.73–7.87), probably due to the proximity of mine tailing disposal sites, which are the source of carbonate particles (Kříbek et al., 2016). However, a slightly elevated C_{inorg} concentration was only observed in sample P6 (19.8 g kg^{-1}; Table 1). In the Zambian soils, the highest S_{tot} concentrations were close to the pollution sources (up to 1250 mg kg^{-1}) and decreased as a function of the distance. In the two Namibian topsoil samples, S_{tot} varied from 411 to 4070 mg kg^{-1}, the latter value found in humified litter, where the highest C_{org} was also observed (241 g kg^{-1}) compared to other samples studied (Table 1).

Contaminant concentrations reflected the compositions of ores mined and processed in individual areas; whereas polluted soils from the Zambian Copperbelt were significantly richer in Cu (up to 8980 mg kg^{-1}) and Co (up to 45.8 mg kg^{-1}). Namibian soils were enriched in Pb (up to 4640 mg kg^{-1}), Zn (up to 2620 mg kg^{-1}), Cd (up to 96.7 mg kg^{-1}), As (up to 1450 mg kg^{-1}), and Sb (95.7 mg kg^{-1}). Vanadium concentrations were similar for both localities and varied in the 20.9 to 41.1 mg kg^{-1} range (Table 1).

The XRD investigation of the heavy mineral fraction indicated the presence of geogenic phases of high density (tourmaline, zircon, rutile/anatase, ilmenite, Fe and Mn oxides) with low amounts of lighter phases (such as quartz, micas, or carbonates), which were not fully separated from the samples in heavy liquids due to their intimate associations with the heavier phases (Table 1). Metal(loid)-bearing phases were detected by XRD only in the most polluted samples (Table 1). The presence of chalcopyrite ($CuFeS_2$) was suggested in the most Cu-enriched soil from Zambia (sample F1); based on relative intensity ratio calculations (RIR) it accounted for 1% of the heavy mineral fraction (see diffraction patterns in Fig. S1 and comparisons with reference data in Table S2 in the Supplementary Material). The presence of galena (PbS; 1%), pyrite (FeS_2; 10%), conichalcite [$CaCu(AsO_4)(OH)$; 14%], and

duftite [$PbCu(AsO_4)(OH)$; 3%] was suggested in the most polluted soil from Namibia (sample P6) (Fig. S1 and Table S2). The presence of fayalite (Fe_2SiO_4) originating from the windblown smelting slag particles was also evidenced in sample P6 by XRD. The presence of amorphous slag glass in this sample was also consistent with an increased background in the diffraction pattern between 15 and 40° 2theta (Fig. S1).

3.2. Morphology of metal(loid)-bearing particles

Along with their chemical composition, the morphology of soil particles is a useful tracer of their origin. Spherical metal(loid)-bearing particles are very frequent in smelter soils, and represent quenched melt droplets emitted by the smelter smokestack (Ettler et al., 2014a; Gregurek et al., 1998, 1999; Henderson et al., 1998; Knight and Henderson, 2006; Lanteigne et al., 2012, 2014; Shukurov et al., 2014). In contrast, irregular particles with frequent oxidised rims correspond to materials not heated to the melting temperature, and are most likely derived from the mining operations (Gregurek et al., 1999; Shukurov et al., 2014).

Despite the fact that the flue gas cleaning technologies in non-ferrous metal smelting operations are supposed to remove >99% of dust from the flue gas (Ettler et al., 2005a; Schlesinger et al., 2011), some portion of particulates can escape from the smelting facilities during periods of filtering inefficiency, which can occur during the furnace turn-on or towards the lifetime end of the fabric filters (which are, for example, currently used for dust abatement in the Tsumeb smelter). Moreover, earlier contamination from periods when flue gas cleaning was not installed at the studied sites must also be taken into account. Temperatures in the smelting process vary from ~1350 °C (lead smelting in the furnace), ~1250 °C (copper matte smelting in the furnace), 1220–1200 °C (copper converting in convertors), down to ~80 °C (flue gas cleaning) (Ettler et al., 2005a; Schlesinger et al., 2011). The offgas from the smelting operations has high temperatures (1100 to 1230 °C based on the smelting technology used); however, it is cooled down within a few seconds in heat recovery boilers to achieve temperatures around 350–400 °C before subsequent flue gas cleaning in electrostatic precipitators (Mufulira) or baghouse filtering facilities (Tsumeb) (Schlesinger et al., 2011).

The microscopic investigations of the heavy mineral fractions from the studied soils indicated that geogenic particles predominantly occurred as angular grains (see the zircons or rutiles in Figs. 2 and 3). In contrast, morphological types of the metal(loid)-bearing particles were quite variable. They included:

(i) Angular grains, from 5 to 150 μm in size, with or without weathering rims, and most likely originating from mining operations or mine tailing disposal sites (Fig. 2a,c, and b, respectively);
(ii) Particles of spherical shapes, ranging from 20 to 150 μm in size, and corresponding to droplets of quenched slag or matte melt, emitted from the smelting furnaces and convertors (Figs. 2e-l and 3a,b,i,l);
(iii) Skeletons of highly weathered metal-rich particles originally formed in the flue-gas cleaning systems of the smelters, generally <50 μm in size (such as delafossite, $Cu^{1+}Fe^{3+}O_2$ in Fig. 2e,g,j,l);
(iv) Irregular grains of smelter slag most likely windblown from the slag disposal sites, generally from 5 to hundreds of μm in size (Fig. 3);
(v) Secondary matrix precipitates presumably formed as fillings between other particulates (Fig. 3g,k).

3.3. Composition and weathering of metal(loid)-bearing particles

Generally, the most polluted soil samples are enriched in metal(loid)-bearing particulates identified by SEM/EDS and EPMA (Table 1). Table 2 summarises groups of individual phases detected at each locality, supplemented with numbers of performed microprobe analyses and suggested origin(s) for each of the identified phases, based on their morphologies and crystal chemistry.

3.3.1. Sulphides and sulphates

At both of the sites studied, metal-bearing sulphides were the most frequent phases (Table 2). Representative EPMA data, with calculated structural formulae of the individual sulphides (plus enargite, Cu_3AsS_4, as an example of a sulphosalt) are given in Table S3 in the Supplementary Material. Chalcopyrite ($CuFeS_2$), galena (PbS), pyrite (FeS_2), and sphalerite (ZnS) were perfectly stoichiometric, and occurred as angular grains with weathering rims (Figs. 2a–d and 3b). They often exhibit original ore textures (Fig. 2b), and most likely correspond to windblown material from mine tailing sites or ore crushers. Similarly, low-temperature sulphides (idaite, Cu_3FeS_4; yarrowite, Cu_9S_8; Fig. 2b) and sulphosalts (enargite; Fig. 3i) with similar grain morphologies most likely had the same origin. However, some of the Cu–Fe sulphides occurred in both mining- and smelter-related particles, and could have either origin. For example, chalcocite (Cu_2S) and bornite (Cu_5FeS_4) either formed ore-derived particles (Fig. 2b and d, respectively) or they occurred as smelter-derived spherical particles, where they were associated to metallic Cu (Fig. 2g,h) or other sulphides (e.g., galena) in the form of a symplectitic intergrowth (Fig. 3f). The latter indicates a rapid eutectic crystallisation, which for the bornite–galena system takes place at 609 °C (Tesfaye and Taskinen, 2011). Covellite (CuS) and digenite (Cu_9S_5) (Figs. 2j and 3a,l) as well as various non-stoichiometric Cu–(Fe) sulphides only occurred as spherical particles, and clearly originated from smelters (Figs. 2e,i and 3b,i). The compositions of the latter were highly variable, and in some cases, submicrometric two-phase intergrowth (symplectites), impossible to be analysed by EPMA, can also occur (Fig. 3i; Table S3 and Fig. S2). All of these phases form at high temperatures (e.g., chalcocite (Cu_2S), and digenite ($Cu_{2-x}S$) with thermal stabilities up to 1130 °C; and covellite (CuS) with thermal stability up to 507 °C) (Chakrabarti and Laughlin, 1983). Similar phases were reported from dusts and snow samples collected near Cu–Ni smelters in NW Russia (Barcan, 2002; Gregurek et al., 1998, 1999), in surface soils near Sudbury Cu–Ni smelters in Canada (Lanteigne et al., 2012, 2014), in dust deposited on grass near the Tsumeb Cu smelter in Namibia (Kříbek et al., 2016), and in dusts directly sampled above the Cu convertors at the Rönnskär copper smelter in Sweden (Samuelsson and Björkman, 1998a).

Oxygen-enriched air is used in the copper converting process (Samuelsson and Björkman, 1998a; Schlesinger et al., 2011). Due to the presence of oxygen in the flue gas stream, complex mixtures of various Cu oxides, sulphides, and sulphates can form, and are often associated with one another, as recently demonstrated in the critical evaluation of the Cu–S–O system (Shishin and Decterov, 2012). Sulphates were often observed in the dusts collected from the flue gas cleaning facilities or smokestacks in non-ferrous metal smelters. For example, anglesite ($PbSO_4$), gunningite ($ZnSO_4 \cdot H_2O$), and Cu sulphates (chalcocyanite ($CuSO_4$) or chalcanthite ($CuSO_4 \cdot 5H_2O$)) were reported from Pb and Cu smelter flue dusts (Ettler et al., 2005a; Morales et al., 2010; Skeaff et al., 2011; Vítková et al., 2011). Dunn and Muzenda (2001), and Simonescu et al. (2007) studied the thermal transformations of covellite (CuS) and described a multi-step process depending on temperature and atmosphere, in which different Cu sulphides ($Cu_{1.8}S$, Cu_2S), oxides (Cu_2O, CuO), sulphates (Cu_2SO_4, $CuSO_4$), and oxysulphates ($CuO \cdot CuSO_4$) may form. Spherical particles composed of symplectitic intergrowths of covellite and non-stoichiometric $CuSO_4$ found in Mufulira soils (Fig. 2e) could result from quenching in the flue gas from the copper converting process in the presence of oxygen (covellite is stable up to 507 °C and $CuSO_4$ is stable below 585 °C; Chakrabarti and Laughlin, 1983; Dunn and Muzenda, 2001). It is also important to note that small amounts of oxygen (<2.82 wt.%) were detected by EDS analysis in the quenched Cu–(Fe) sulphides (see analyses

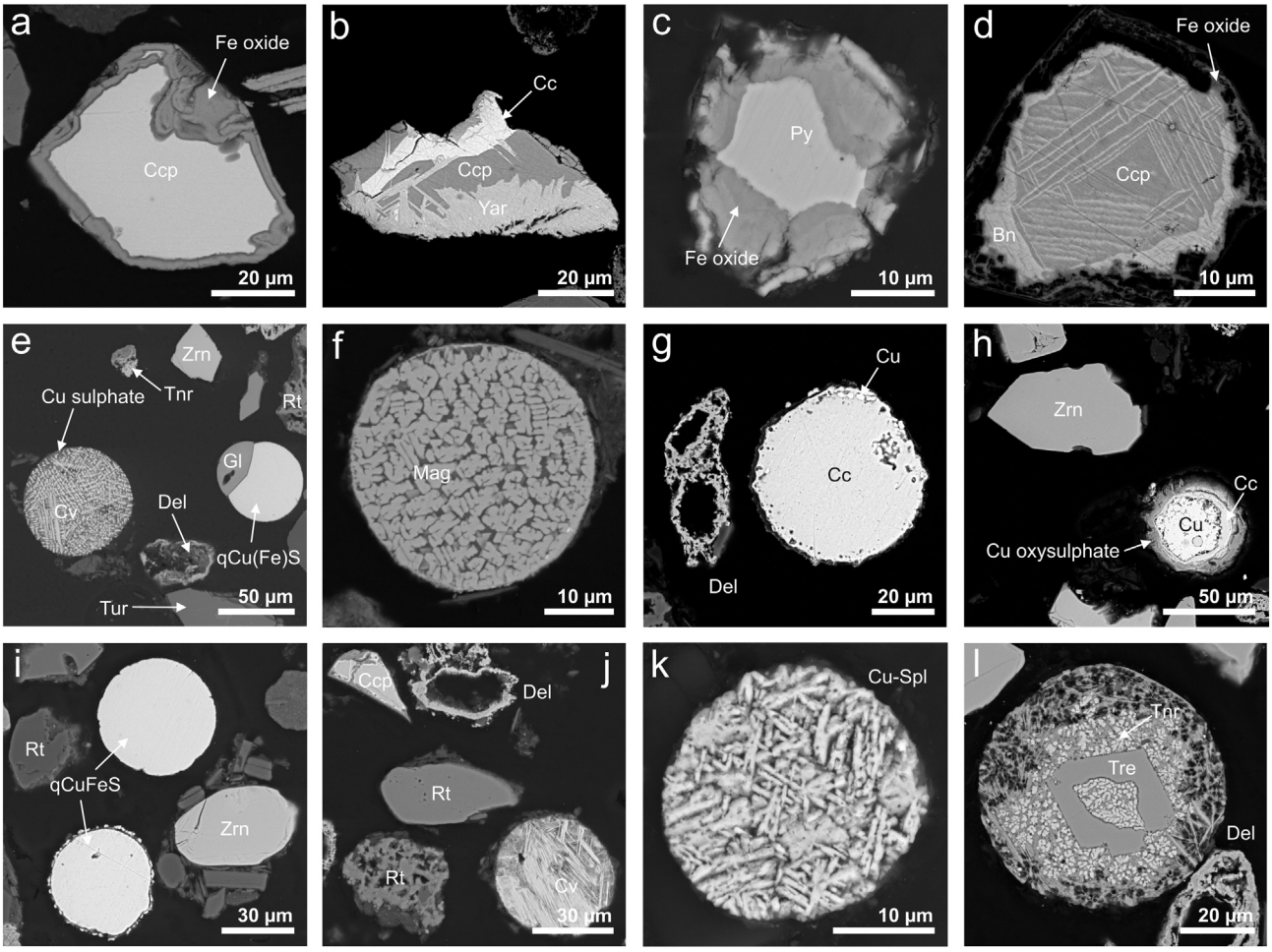

Fig. 2. Scanning electron micrographs in back-scattered electrons (BSE) of heavy particulates from mining- and smelting-affected humid subtropical soils (Mufulira, Copperbelt, Zambia). a) Chalcopyrite with weathered rim composed of Fe oxide (origin: mine tailing); b) Ore mineral particle composed of the association of chalcocite, yarrowite, and chalcopyrite (origin: mine tailing); c) Pyrite grain with weathered Fe-oxide rim (origin: mine tailing); d) Ore mineral particle composed of chalcopyrite associated with bornite (origin: mine tailing); e) Spherical covellite particle with weathered Cu sulphate, sphere of quenched Cu–(Fe)–S compound associated with slag glass, and weathered delafossite and tenorite grains (origin: smelter); f) Spherical particle composed of magnetite (origin: smelter); g) Spherical particle of chalcocite with inclusions of Cu metal and skeleton of weathered delafossite particle (origin: smelter); h) Metallic Cu with weathered rim composed of Cu-(oxy)sulphate (origin: smelter); i) Spheres of quenched Cu–Fe–S compounds (origin: smelter); j) Chalcopyrite grain (origin: mine tailing), spherical particle of covellite and collapsed structures of weathered delafossite (origin: smelter); k) Spherical particle of cuprospinel (origin: smelter); l) Spherical particle composed of a residual trevorite grain surrounded by weathered myrmekite of trevorite and tenorite (origin: smelter). Abbreviations: Bn — bornite (Cu_5FeS_4), Cc — chalcocite (Cu_2S), Ccp — chalcopyrite ($CuFeS_2$), Cu — metallic copper (Cu), Cu-Spl — cuprospinel ($CuFe_2O_4$), Cv — covellite (CuS), Del — delafossite ($CuFeO_2$), Gl — glass (slag), Mag — magnetite (Fe_3O_4), Py — pyrite (FeS_2), qCuFeS — quenched phase in the Cu–Fe–S system, Rt — rutile (TiO_2), Tn — tenorite (CuO), Tre — trevorite ($NiFe_2O_4$), Tur — tourmaline (mainly schorl: $NaFe_3Al_6Si_6O_{18}(BO_3)_3(OH)_4$), Yar — yarrowite ($Cu_9S_8$), Zrn — zircon ($ZrSiO_4$).

in Table S3). These results are in agreement with the modelling work of Shishin and Decterov (2012), who suggested that based on previous measurements <0.2 mol% (i.e., 3.2 wt.%) oxygen can be trapped in the Cu sulphide matte.

We believe that the intimate association of Cu sulphides and sulphates along with the oxygen content in the Cu–Fe–S phases, as described above, is not related to any weathering processes in soils. Our observations indicate that sulphates formed by weathering are very rare in soils from either of the studied locations. We observed only one diffuse weathering rim of complex Cu (oxy)sulphates on Cu sulphides and metallic phases (Fig. 2h; EPMA in Table S5), and anglesite ($PbSO_4$)-like rims on galena crystals (Fig. 3b). It is also important to note that except for the relatively stable anglesite, which has been detected in temperate soils near Pb smelters (e.g., Ettler et al., 2005b), other simple (oxy)sulphates were practically not observed in the studied soils despite their presence in the original smelter dusts. This observation is probably related to their relatively high solubility. For example, ESP dust from the Mufulira Cu smelter contained chalcanthite, which rapidly dissolved in contact with water during leaching tests, and partly transformed to antlerite ($Cu_3(SO_4)(OH)_4$) (Vítková et al., 2011; Ettler et al., 2014b), which, however, is also not very stable from a long-term perspective (Yoder et al., 2007). Similarly, if chalcocyanite is present in the smelter dust, it quickly disappears when leached in water (Morales et al., 2010; Skeaff et al., 2011).

3.3.2. Oxides

Oxides were also important metal(loid)s carriers in the studied soils, with higher frequencies of occurrence in samples from the Zambian Copperbelt (Table 2; EPMA data in Table S4 in the Supplementary Material). Shishin et al. (2013) investigated the Cu–Fe–O system using thermodynamic modelling, and found that various spinel phases associated with metallic copper, tenorite (CuO), and delafossite could form at temperatures below 1154 °C. Tenorite occurred either as small (<20 μm) grains, which could have a smelter origin and/or be formed by transformation/weathering in the soil (Fig. 2e); or formed as biphase spherical particles up to 60 μm in size, where tenorite was partly dissolved and trevorite ($NiFe_2O_4$) formed an unweathered skeleton (Fig. 2l). Besides trevorite, other spinel-family phases occurred in spherical particles: magnetite ($Fe^{2+}Fe^{3+}{}_2O_4$) associated with glass in slag-like inclusions (Fig. 2f), and cuprospinel (with a composition

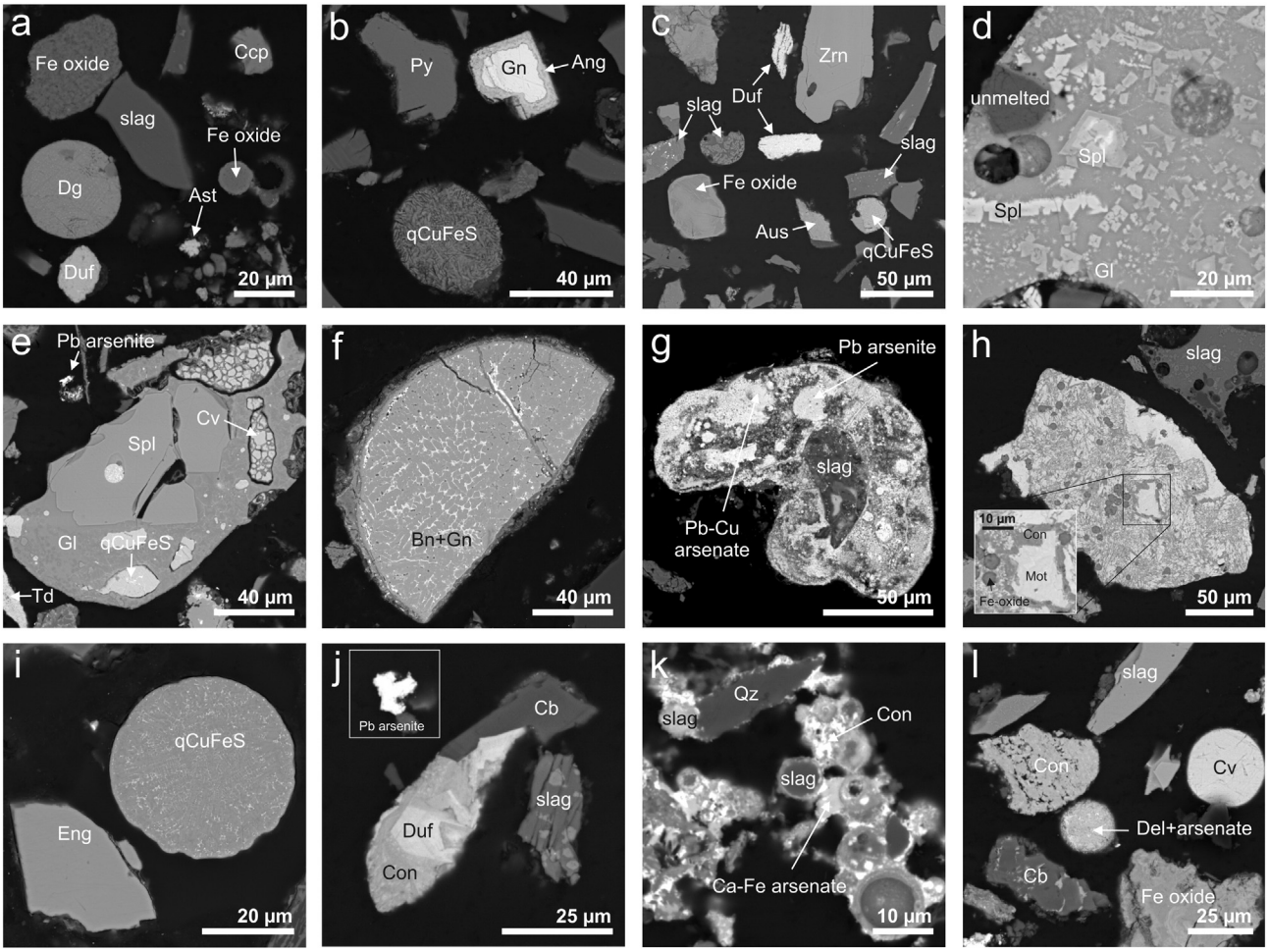

Fig. 3. Scanning electron micrographs in back-scattered electrons (BSE) of heavy particulates from mining- and smelting-affected semi-arid soils (Tsumeb, Namibia). a) Spherical digenite particle and slag glass (origin: smelter) associated with chalcopyrite, duftite and arsentsumebite grains (origin: mine tailing); b) Spherical particle of quenched Cu–Fe–S compound (origin: smelter), and angular grains of pyrite and weathered galena (origin: mine tailing); c) Angular grains of duftite and austinite (origin: mine tailing), associated to slag grains and a sphere of quenched Cu–Fe–S phase (origin: smelter); d) Slag particle composed spinel crystals and unmelted silicate grain entrapped within glass (origin: smelter); e) Smelter slag particle composed of spinel and glass with inclusions of quenched Cu–Fe–S phase and weathered covellite (origin: smelter), associated with Pb arsenite (origin: mine tailing) and newly formed Pb-bearing todorokite; f) Matte particle composed of bornite–galena myrmekite (origin: smelter); g) Lead arsenite and Pb–Cu arsenate phases associated to weathered slag grain (origin: smelter, weathering in soil?); h) Slag fragment (origin: smelter) and grain composed of mottramite, conichalcite and Fe oxide (zoom inset) (origin: mine tailing); i) Angular grain of enargite (origin: mine tailing), and spherical particle of quenched Cu–Fe–S phase (origin: smelter); j) Ore grain composed of conichalcite, duftite and gangue carbonate with weathered Pb arsenite grain (inset) (origin: mine tailing), associated to weathered slag particle (origin: smelter); k) Spherical smelter slag particles and angular grain of quartz cemented with conichalcite and Ca–Fe arsenate phase; l) Sphere of covellite and delafossite/arsenate mixture (origin: smelter), and angular grains of conichalcite (origin: mine tailing) associated with carbonate and Fe oxide. Abbreviations: Ang — anglesite ($PbSO_4$), Ast — arsentsumebite ($Pb_2Cu(AsO_4)(SO_4)(OH)$), Aus — austinite ($CaZn(AsO_4)(OH)$), Bn — bornite (Cu_5FeS_4), Cb — carbonate (variable composition); Ccp — chalcopyrite ($CuFeS_2$), Con — conichalcite ($CaCu(AsO_4)(OH)$), Cv — covellite (CuS), Del – delafossite ($CuFeO_2$), Duf — duftite ($PbCu(AsO_4)(OH)$), Eng — enargite (Cu_3AsS_4), Gn — galena (PbS), Mot — mottramite ($PbCu(VO_4)OH$), Py — pyrite (FeS_2), qCuFeS — quenched phase in the Cu–Fe–S system, Sp — sphalerite (ZnS), Spl — spinel (variable composition), Td — todorokite ($Pb_{1-x}Mn_6O_{12}$).

close to $[Cu,Fe^{2+}]Fe^{3+}{}_2O_4$; Fig. 1k). High-temperature spinel phases (magnetite, Cu- and Ni-bearing spinels) have frequently been described in smelter dusts (Ettler et al., 2014b; Morales et al., 2010; Vítková et al., 2011), in polluted soils and snowpack samples, and in weathering crusts on rocks near numerous non-ferrous metal smelters (Cabala and Teper, 2007; Caplette et al., 2015; Gregurek et al., 1998, 1999; Lanteigne et al., 2012, 2014; Mantha et al., 2012; Shukurov et al., 2014). In agreement with observations by other authors (Adamo et al., 1996; Cabala and Teper, 2007; Gregurek et al., 1999; Knight and Henderson, 2006; Lanteigne et al., 2012, 2014; Shukurov et al., 2014), skeletal textures of oxides in these spherical particles indicate a rapid cooling regime in the flue gas stream (Fig. 2f,k,l). As a result, they clearly correspond to quenched droplets of slag formed during smelting and converting (Samuelsson and Björkman, 1998a; Schlesinger et al., 2011).

Delafossite ($Cu^{1+}Fe^{3+}O_2$) is a common phase in the Cu smelter dusts (Ettler et al., 2014b; Morales et al., 2010; Vítková et al., 2011) and it was also the most frequent oxide phase observed in humid subtropical soils from Mufulira. Despite the fact that delafossite was found to be rather stable during the short-term leaching of smelter dusts (Vítková et al., 2011; Ettler et al., 2014b), its "collapsed skeleton" grains, separated from soil samples (Fig. 2e,g,j,l), indicate that it underwent intensive weathering, and had similar morphologies as the weathered grains of oxides in smelter soils from the Sudbury area as described by Lanteigne et al. (2012).

Angular sulphides frequently have weathering rims composed of hydrous ferric oxides (Fig. 2a,c,d) similar to those observed in mine tailing dumps (cf. Jamieson, 2011 and references therein). Moreover, distinct grains of metal(loid)-rich haematite (Fe_2O_3) (Fig. 3a) and Mn oxides (such as todorokite with a composition close to $Pb_{1-x}Mn_6O_{12}$; Fig. 3e; and analyses 4/1 and 39/1 in Table S4) were also identified. We assume that they probably formed by natural transformation processes in the soils.

3.3.3. Other phases

Windblown slag-like Si-rich particles were reported from numerous Cu smelting sites (Barcan, 2002; Chopin and Alloway, 2007; Gregurek

Table 2
Metal-bearing phases detected in the heavy mineral fraction of the studied soils (n = number of EPMA analyses).

Group	Phase	Formula	n (Mufulira)	n (Tsumeb)	Origin
Sulphides and sulphosalts	Chalcopyrite	$CuFeS_2$	16	5	Mine tailings
	Chalcocite	Cu_2S	11		Mine tailings/smelter
	Covellite	CuS	9	2	Smelter
	Quenched phase	Cu–Fe–S	16	3	Smelter
	Idaite	Cu_3FeS_4	1		Mine tailings
	Yarrowite	Cu_9S_8	1		Mine tailings
	Bornite	Cu_5FeS_4	2	2	Mine tailings/smelter
	Digenite	Cu_9S_5	1	3	Smelter
	Pyrite	FeS_2	1	2	Mine tailings
	Pyrrhotite	$Fe_{1-x}S$		1	Smelter
	Sfalerite	ZnS		1	Mine tailings
	Enargite	Cu_3AsS_4		1	Mine tailings
	Galena	PbS		2	Mine tailings
Metals	Cu metal	Cu	5		Smelter
Oxides	Tenorite	CuO	5		Smelter/transformation in soil
	Delafossite	$CuFeO_2$	13	1	Smelter
	Haematite	Fe_2O_3[a]	4	2	Transformation in soil
	Todorokite	$Pb_{1-x}Mn_6O_{12}$		1	Transformation in soil
	Cuprospinel	$CuFe_2O_4$	4		Smelter
	Magnetite	Fe_3O_4[b]	3		Smelter
	Trevorite	$NiFe_2O_4$	2		Smelter
Sulphates	Cu (oxy)sulphates	$CuSO_4 \cdot CuO/CuSO_4$	2		Smelter/transformation in soil
	Anglesite	$PbSO_4$		1	Transformation in soil
Arsenates	Conichalcite	$CaCu(AsO_4)(OH)$		7	Mine tailings
	Duftite	$PbCu(AsO_4)(OH)$		4	Mine tailings
	Austinite	$CaZn(AsO_4)(OH)$		1	Mine tailings
	Arsentsumebite	$Pb_2Cu(AsO_4)(SO_4)(OH)$		1	Mine tailings
	Unidentified arsenates	(Ca–Pb–Cu–Fe–As–O)		2	Mine tailings
Arsenites	Pb-arsenite	$Pb_4As_2O_7$		5	Mine tailings
Vanadates	Mottramite	$PbCu(VO_4)(OH)$		4	Mine tailings

[a] metal-bearing oxides (products of weathering/transformation in soils).
[b] metal-bearing magnetite originating from the smelting process (slag-like materials).

et al., 1999; Knight and Henderson, 2006). Despite the fact that disposal sites near the Mufulira smelter also contained granulated slags (Kříbek et al., 2010; Vítková et al., 2010), no windblown slag particles from slag dumps have been observed in the studied soils due to the relatively large distance from the smelter (>3.6 km). In contrast, Tsumeb soil samples are rich in slag particles of various sizes. At this site, milled slag material, after re-flotation and heavy fraction recovery, is used to cover mine tailing disposal sites; additionally, numerous dumps of old granulated slag are located in the area (Ettler et al., 2009; Kříbek et al., 2016). The mineralogy of the slag particles from soils corresponds well to slags previously studied from this area (detailed by Ettler et al. (2009)), with predominant skeletal and dendritic crystals of spinels and silicates entrapped within the glass (Fig. 3). While at other sites slag particles were found to be quite resistant to weathering (Chopin and Alloway, 2007), our microscopic observations clearly indicate that some of them were partly chemically and/or mechanically weathered (Fig. 3e,j).

Arsenic is a key contaminant in smelter dusts especially in smelters where As-rich concentrates are processed, as is the case at the Tsumeb Cu smelter. Based on thermodynamic modelling and analysis of chemical and mineralogical composition of dusts from the copper converting process, Samuelsson and Björkman (1998a, 1998b) suggested that As_2O_5 should form if 5 to 100% of air has been added to the system. However, arsenolite (As_2O_3) was described as the most common As-bearing phase in smelter dusts, formed by precipitation from the volatile form as the flue gas is rapidly cooled (Majzlan et al., 2014 and references therein; Morales et al., 2010; Schlesinger et al., 2011; Skeaff et al., 2011). Minute arsenolite grains originating from the smelter dust were also found on the surface of grasses collected in the Tsumeb area (Kříbek et al., 2016). However, we never detected any arsenolite particles in the collected As-rich soil samples from Tsumeb (up to 1450 mg As kg^{-1}). Due to the high solubility of arsenolite, which has been experimentally established (Morales et al., 2010; Skeaff et al., 2011; Yue and Donahoe, 2009), we hypothesise that if initially present it has been completely dissolved/transformed when deposited in soils. A large variety of other As-bearing phases have been identified in the soil heavy mineral fractions; conichalcite [$CaCu(AsO_4)(OH)$] and duftite [$PbCu(AsO_4)(OH)$] were the most frequently observed, and were detected by both XRD and EPMA. Conichalcite, duftite, and other less abundant arsenates such as arsentsumebite [$Pb_2Cu(AsO_4)(SO_4)(OH)$] and austinite [$CaZn(AsO_4)(OH)$] generally formed angular grains (Fig. 3a,c,j,l) and were often associated with gangue minerals (carbonates, Fig. 3j). Similar grain morphologies were observed for the relatively rare particles of mottramite [$PbCu(VO_4)(OH)$] (Fig. 3h; analysis 2/1 in Table S5). We believe that the arsenates and vanadates mainly correspond to particulate matter formed during mining activities as they are also found within the ore minerals from the Tsumeb deposit (as recently summarised by Bowell (2014)).

Nevertheless, conichalcite and other unidentified Pb–Cu and Ca–Fe arsenates also occurred as fillings between slag grains and other phases (Fig. 3g,k). It is important to mention again that old slags resulting from historic smelting technologies at Tsumeb were highly weathered and contained secondary metal-arsenates (Ettler et al., 2009), and these could potentially also be present in the studied soils located near slag disposal sites. However, these arsenates could also be weathering/transformation products formed in the soils. Gutiérrez-Ruiz et al. (2012) identified Ca-arsenate [$Ca_5(AsO_4)_3(OH)$] in an alkaline carbonate-rich smelter waste deposited in soils near a Pb smelter area in Mexico. In soils with high metal(loid) concentrations (6043 mg As kg^{-1}, 31,420 mg Pb kg^{-1}, 12,280 mg Zn kg^{-1}, 553 mg Cu kg^{-1}), high-resolution transmission electron microscopy (HRTEM) indicated the occurrence of composed of duftite, arsentsumebite, arsenbrackebuschite [$Pb_2(Fe,Zn)(AsO_4)_2(OH,H_2O)$], and hydroxymimetite [$Pb_5(AsO_4)_3(OH)$]. Based on their analytical data and geochemical modelling, Gutiérrez-Ruiz et al. (2012) suggested that the in-gassing of atmospheric CO_2 slowly decreased the alkalinity of these soils, which resulted in the dissolution of Ca arsenates and the precipitation of secondary Pb-bearing arsenates. Geochemical modelling further indicated that duftite would be stable over a large pH range (4–10) (Gutiérrez-Ruiz et al., 2012). A similar

mechanism could be proposed for the Tsumeb soils, where As, initially released by arsenolite dissolution in soil, could react at circumneutral pH with metallic ions (Pb, Cu, Ca), leading to precipitation of relatively stable metal-bearing arsenates.

In addition, numerous unknown arsenites with perfect stoichiometry close to $Pb_4As_2O_7$ have been observed. They occur either as small irregular grains (Fig. 3e,j) or parts of complex particles composed of arsenates and residual slag grains (Fig. 3g) (analyses 10/1 and 16/1 in Table S5). Their origin is unknown, but we hypothesise that at least some of them could be transported from mining operations (ore crushers, mine tailings), because rare metal arsenites were also found in the Tsumeb ores (Bowell, 2014).

3.4. Metal(loid) availability and environmental implications

Relatively high concentrations corresponding to the "labile" fraction of Cu have been found in polluted soils from the Zambian Copperbelt (1230–3500 mg kg^{-1}) (Table 3). In the case of Cu, this fraction accounted for 22.6–55.5% of the total concentration, indicating its high (bio)availability. Interestingly, reference samples from this area also exhibited a high percentage of "labile" fraction, but total concentrations were 2 orders of magnitude lower than at sites closer to the smelter (Tables 1 and 3). Compared to Cu, total concentrations and the "labile" fraction of other metals (Co, Pb, Zn, V) were significantly lower and Cd, As, and Sb were not detected in most of the Zambian samples (Tables 1 and 3). Similarly, a high proportion of "available/exchangeable" Cu was detected in Oxisols sampled near a Cu smelter in Kitwe (Zambia) (Ettler et al., 2011). An increase in the "labile" fraction of Cu (up to 75% of the total concentration) was recently documented experimentally in an Oxisol artificially polluted with Cu smelter fly ash and subjected to laboratory weathering in a pot experiment (Ettler et al., 2016). The ESP dust from the Cu smelter in Mufulira is mainly composed of delafossite, magnetite, Cu spinel, and chalcanthite (Vítková et al., 2011; Ettler et al., 2014a, 2014b); with the latter phase, being highly soluble, responsible for the major release of Cu into the soil system. Due to the fact that (sub)tropical soils generally exhibit low organic matter content, and contain kaolinite and haematite (both minerals with a relatively low sorption capacity), they are more vulnerable to pollution when compared to temperate soils, which exhibit a higher retention potential for inorganic contaminants (Ettler (2016) and references therein). Our study shows that practically no Cu sulphates were found in the heavy mineral fractions of the soils from the Zambian Copperbelt; therefore, it is evident that these phases were highly reactive when smelter dust was deposited onto the soil and interacted with soil pore water and soil components; and that Cu released by their dissolution subsequently fractionated into the "labile" pool. Interestingly, our microscopic observations indicate that smelter-derived sulphides forming spherical particles seem to be relatively resistant to weathering. In contrast to previous study conducted in the Mufulira area (Ettler et al., 2014a), our detailed mineralogical investigation indicates that Cu-bearing oxides (Cu spinels and delafossite) were highly weathered, and probably also contributed to the relatively high proportion of "labile" Cu in the studied subtropical soils.

In contrast, despite high concentrations of all of the studied metal(loid)s in the Tsumeb semi-arid soils, their "labile" fractions were rather low, ranging from 0.2% (V) to 5.6% (Cd) of the total concentration. This observation clearly indicates that the amount of potentially available metal(loid)s is quite limited, and they were probably efficiently immobilised in the soil. The reason for this finding may be partly related to the high proportion of non-weathered metal(loid)-rich slag particles, windblown from nearby slag disposal sites. Chopin and Alloway (2007) showed that trace elements were predominantly bound in the residual (i.e., the least available) fraction in soils, and enriched in metal(loid)-bearing slag fragments. Moreover, they concluded that the slag particles were not transported over long distances from the disposal sites, and that the resulting spatial impacts on the surrounding environment were minimal (Chopin and Alloway, 2007). The low availability of metal(loid)s in the Tsumeb soils may also be governed by the nearly-neutral or slightly alkaline conditions (pH = 6.73–7.87). Geochemical modelling and observations at other smelting sites in semi-arid areas indicated that metal-bearing arsenates are quite stable under these conditions and efficiently control the mobility of As and metals (Cu, Pb) (Gutiérrez-Ruiz et al., 2012). The same "attenuation" mechanisms for Cu, Pb, and As can be suggested for highly polluted Tsumeb soils.

The size of the metal(loid)-bearing particulates/particles, along with wind speeds and directions, are the key parameters affecting the distribution of contaminants in the environments near mining and smelting operations (Csavina et al., 2012 and references therein; Kříbek et al., 2010, 2016). Smaller aerosols and dust particles can travel over greater distances from the pollution source. Moreover, Csavina et al. (2014) recently demonstrated that the finest sized fraction (<1 μm) of dust and aerosols is significantly richer in metal(loid)s than are the coarser fractions. For example, dusts and aerosols collected near the Hayden copper smelter in Arizona contained 88% and 86% of the As and Pb in the fine dust fraction (<1 μm), respectively. The reason for the higher proportion of "labile" fractions of metal(loid)s in subtropical soils compared to semi-arid ones (observed in this study) may also be related to the higher rate of contaminant scavenging by precipitation events in the subtropical area. Schindler et al. (2012) and Sorooshian et al. (2012) hypothesised that especially the smelter-derived metal-sulphate aerosols, which are commonly found in the smallest size fractions, might be efficiently scavenged by rain, subsequently limiting the spatial influence of transported aerosols on the downwind regions.

The accurate mineralogical analysis of ultrafine particles emitted by non-ferrous metal smelters is still a challenge for the future, and the application of high-resolution techniques (HRTEM) is definitely needed. The separation of such fine particles from soils located at greater distances from the pollution source, and their subsequent specimen preparation and analysis, is virtually impossible – and the only realistic way

Table 3
Concentrations of "labile" fractions of metal(loid)s in individual samples (in mg kg^{-1} as obtained by EDTA extraction), and corresponding percentage of the total amount (mean values, $n = 2$).

Sample	Cu mg kg^{-1} (%)	Co mg kg^{-1} (%)	Pb mg kg^{-1} (%)	Zn mg kg^{-1} (%)	Cd mg kg^{-1} (%)	As mg kg^{-1} (%)	Sb mg kg^{-1} (%)	V mg kg^{-1} (%)
Subtropical soils								
F1	3500 (39.0)	5.50 (12.0)	10.5 (25.2)	7.35 (11.6)	nd	0.17 (3.3)	nd	0.36 (1.0)
E1	1570 (55.5)	7.68 (36.5)	8.77 (41.2)	19.7 (30.3)	nd	0.07 (1.1)	nd	0.96 (1.7)
A1	1240 (22.6)	1.07 (4.3)	4.60 (11.8)	1.31 (1.6)	nd	nd	nd	0.76 (1.3)
O1	1230 (37.0)	5.50 (23.5)	5.85 (32.7)	6.78 (13.4)	nd	nd	nd	0.66 (3.1)
G1	12.0 (32.2)	0.60 (22.4)	nd	5.29 (21.0)	nd	nd	nd	0.43 (1.8)
H1	15.4 (42.2)	0.83 (30.4)	0.96 (22.2)	1.69 (10.9)	nd	nd	nd	0.31 (1.5)
Semi-arid soils								
P1	9.05 (2.6)	0.06 (1.1)	15.3 (3.9)	3.51 (1.3)	0.38 (5.6)	1.20 (1.3)	0.03 (0.5)	0.07 (0.2)
P6	156 (3.5)	0.11 (0.8)	197 (4.3)	48.0 (1.8)	3.36 (3.5)	24.5 (1.7)	0.33 (0.3)	0.09 (0.2)

nd – not detected.

is to study the alteration layers on the rocks (Caplette et al., 2015; Mantha et al., 2012; Schindler et al., 2012), or those particles preserved in snow samples (Gregurek et al., 1998, 1999), which are only restricted to certain regions.

Our results have significant implications for the agricultural practices in the two studied areas. Due to the significantly higher metal(loid) availability in soils, the risk of contaminant uptake by crops is much higher in the Zambian Copperbelt, and this agrees well with data reported by Kříbek et al. (2014a, 2014b) for cassava (*Manihot esculenta*) cultivated in this area. However, it must be stressed that the windblown metal(loid)-rich dust particles deposited on foliage remain the major source of contamination of agricultural crops, rather than contaminants translocation from soils via the root system (Kříbek et al., 2014a, 2014b).

4. Conclusions

The heavy mineral fractions separated from mining- and smelter-affected topsoils, located in both a humid subtropical area (Mufulira, Zambian Copperbelt) and in a hot semi-arid area (Tsumeb, Namibia) were studied. The highest concentrations of inorganic contaminants in the bulk soils were: 1450 mg As kg^{-1}, 8980 mg Cu kg^{-1}, 4640 mg Pb kg^{-1}, and 2620 mg Zn kg^{-1}. Using the combination of XRD, SEM/EDS, and EPMA, numerous anthropogenic metal(loid)-bearing particles smaller than 200 μm were identified in these soils. Whereas the spherical metal(loid)-bearing particles resulted from the smelting and flue gas cleaning processes, the angular particles were most likely windblown from the mining operations and disposal sites. At both localities, sulphides from ores and mine tailings (e.g., chalcopyrite, galena) often exhibited weathering rims. In contrast, smelter-derived high-temperature sulphides (chalcocite, digenite, covellite, non-stoichiometric quenched Cu–Fe–S phases) forming spherical particles did not exhibit any significant alteration. Weathering features were more frequently found in samples from humid subtropical areas, where especially copper-bearing oxides (e.g., delafossite) occurred as highly weathered skeletal grains. A high proportion of "labile" fractions of metal(loid)s were reported for soils from humid subtropical areas (up to 55% of total Cu). This finding is probably related to the higher dissolution rate of smelter dusts (predominantly composed of soluble chalcanthite and delafossite) after their deposition in soils, and higher rates of wet scavenging of metal-sulphate aerosols during rain events. In contrast, metal(loid)s were efficiently retained in semi-arid soils and their "labile" concentrations were significantly lower (<6% of the total) than in subtropical soils. This phenomenon is probably related to metal(loid) binding in non-weathered smelter slag particles, windblown from slag disposal sites, and the frequent occurrence of the low-solubility complex Ca–Cu–Pb arsenates (e.g., conichalcite, duftite), which can be windblown from mining operations or precipitated directly in the soils. Due to the higher availability of contaminants and lower stability of metal(loid)-bearing particles in subtropical soils, a higher potential risk for contaminant uptake by agricultural crops in the Zambian Copperbelt can be expected.

Acknowledgements

Support from the Czech Science Foundation (project no. 13-17501S) is acknowledged. The corresponding author's team was also supported by the Operational Programme Prague - Competitiveness (project no. CZ.2.16/3.1.00/21516). A number of colleagues helped with the analytical work: Petr Drahota (XRD and fruitful discussions), Martin Racek (SEM/EDS), Zuzana Korbelová (SEM/EDS, EPMA), Marie Fayadová (digestions and extractions). Peter Lemkin is thanked for reviewing the English manuscript. The thorough reviews of three anonymous reviewers helped to improve the original version of the manuscript.

Appendix A. Supplementary data

contains QC/QA data, selected XRD results, and EPMA data with structural formulae of individual metal(loid)-bearing phases from mining- and smelter-polluted soils (5 tables and 2 figures). Supplementary data associated with this article can be found in the online version, at http://dx.doi.org/10.1016/j.scitotenv.2016.04.133.

References

Adamo, P., Dudka, S., Wilson, M.J., McHardy, W.J., 1996. Chemical and mineralogical forms of Cu and Ni in contaminated soils from the Sudbury mining and smelting region, Canada. Environ. Pollut. 91, 11–19. http://dx.doi.org/10.1016/0269-7491(95)00035-P.

Barcan, V., 2002. Nature and origin of multicomponent aerial emissions of the copper-nickel smelter complex. Environ. Int. 28, 451–456. http://dx.doi.org/10.1016/S0160-4120(02)00064-8.

Bowell, R.J., 2014. Hydrogeochemistry of the Tsumeb Deposit: Implications for Arsenate Mineral Stability. In: Bowell, R.J., Alpers, C.N., Jamieson, H.E., Nordstrom, D.K., Majzlan, J. (Eds.), Arsenic: Environmental Geochemistry, Mineralogy and Microbiology. Reviews in Mineralogy & Geochemistry Vol. 79, pp. 589–627.

Cabala, J., Teper, J., 2007. Metalliferous constituents of rhizosphere soils contaminated by Zn–Pb mining in southern Poland. Water Air Soil Pollut. 178, 351–362. http://dx.doi.org/10.1007/s11270-006-9203-1.

Caplette, J.N., Schindler, M., Kyser, T.K., 2015. The black rock coatings in Rouyn-Noranda, Québec: fingerprints of historical smelter emissions and the local ore. Can. J. Earth Sci. 52, 952–965. http://dx.doi.org/10.1139/cjes-2015-0064.

Chakrabarti, D.J., Laughlin, D.E., 1983. The Cu–S (copper–sulfur) system. Bull. Alloy Phase Diagr. 4, 254–271.

Chopin, E.I.B., Alloway, B.J., 2007. Trace element partitioning and soil particle characterization around mining and smelting areas at Tharsis, Ríotinto and Huelva, SW Spain. Sci. Total Environ. 373, 488–500. http://dx.doi.org/10.1016/j.scitotenv.2006.11.037.

Csavina, J., Landázuri, A., Wonaschütz, A., Rine, K., Rheinheimer, P., Barbaris, B., et al., 2011. Metal and metalloid contaminants in atmospheric aerosols from mining operations. Water Air Soil Pollut. 221, 145–157. http://dx.doi.org/10.1007/s11270-011-0777-x.

Csavina, J., Field, J., Taylor, M.P., Gao, S., Landázuri, A., Betterton, E.A., et al., 2012. A review on the importance of metals and metalloids in atmospheric dust and aerosol from mining operations. Sci. Total Environ. 433, 58–73. http://dx.doi.org/10.1016/j.scitotenv.2012.06.013.

Csavina, J., Taylor, M.P., Félix, O., Rine, K.P., Sáez, A.E., Betterton, E.A., 2014. Size-resolved dust and aerosol contaminants associated with copper and lead smelting emissions: implications for emission management and human health. Sci. Total Environ. 493, 750–756. http://dx.doi.org/10.1016/j.scitotenv.2014.06.031.

Dunn, J.G., Muzenda, C., 2001. Thermal oxidation of covellite (CuS). Thermochim. Acta 369, 117–123. http://dx.doi.org/10.1023/A:1011513616930.

Ettler, V., 2016. Soil contamination near non-ferrous metal smelters: a review. Appl. Geochem. 64, 56–74. http://dx.doi.org/10.1016/j.apgeochem.2015.09.020.

Ettler, V., Johan, Z., Barronnet, A., Jankovský, F., Gilles, C., Mihaljevič, M., et al., 2005a. Mineralogy of air-pollution-control residues from a secondary lead smelter: environmental implications. Environ. Sci. Technol. 39, 9309–9316. http://dx.doi.org/10.1021/es0509174.

Ettler, V., Vaněk, A., Mihaljevič, M., Bezdička, P., 2005b. Contrasting lead speciation in forest and tilled soils heavily polluted by lead metallurgy. Chemosphere 58, 1449–1459. http://dx.doi.org/10.1021/es0509174.

Ettler, V., Johan, Z., Kříbek, B., Šebek, O., Mihaljevič, M., 2009. Mineralogy and environmental stability of slags from the Tsumeb smelter, Namibia. Appl. Geochem. 24, 1–15. http://dx.doi.org/10.1016/j.apgeochem.2008.10.003.

Ettler, V., Mihaljevič, M., Kříbek, B., Majer, V., Šebek, O., 2011. Tracing the spatial distribution and mobility of metal/metalloid contaminants in Oxisols in the vicinity of the Nkana copper smelter, Copperbelt province, Zambia. Geoderma 164, 73–84. http://dx.doi.org/10.1016/j.geoderma.2011.05.014.

Ettler, V., Konečný, L., Kovářová, L., Mihaljevič, M., Šebek, O., Kříbek, B., et al., 2014a. Surprisingly contrasting metal distribution and fractionation patterns in copper smelter-affected tropical soils in forested and grassland areas (Mufulira, Zambian Copperbelt). Sci. Total Environ. 473, 117–124. http://dx.doi.org/10.1016/j.scitotenv.2013.11.146.

Ettler, V., Vítková, M., Mihaljevič, M., Šebek, O., Klementová, M., Veselovský, F., et al., 2014b. Dust from Zambian smelters: mineralogy and contaminant bioaccessibility. Environ. Geochem. Health 36, 919–933. http://dx.doi.org/10.1007/s10653-014-9609-4.

Ettler, V., Petráňová, V., Vítková, M., Mihaljevič, M., Šebek, O., Kříbek, B., 2016. Reactivity of fly ash from copper smelters in an Oxisol: implications for smelter-polluted soil systems in the tropics. J. Soils Sediments 16, 115–124. http://dx.doi.org/10.1007/s11368-015-1174-7.

Gee, G.W., Or, D., 2002. Particle-size analysis. In: Dane, J.H., Topp, G.C. (Eds.), Methods of Soil Analysis, Part 4 — Physical Methods. Soil Science Society of America, Madison, pp. 255–294.

Gražulis, S., Daškevič, A., Merkys, A., Chateigner, D., Lutterotti, L., Quirós, M., et al., 2012. Crystallography Open Database (COD): an open-access collection of crystal structures and platform for world-wide collaboration. Nucleic Acids Res. 40, D420–D427. http://dx.doi.org/10.1093/nar/gkr900.

Gregurek, D., Reimann, C., Stumpfl, E.F., 1998. Mineralogical fingerprints of industrial emissions — an example from Ni mining and smelting on the Kola Peninsula, NW Russia. Sci. Total Environ. 221, 189–200. http://dx.doi.org/10.1016/S0048-9697(98)00293-9.

Gregurek, D., Melcher, F., Pavlov, V.A., Reimann, C., Stumpfl, E.F., 1999. Mineralogy and mineral chemistry of snow filter residues in the vicinity of the nickel–copper

processing industry, Kola Peninsula, NW Russia. Mineral. Petrol. 65, 87–111. http://dx.doi.org/10.1007/BF01161578.
Gutiérrez-Ruiz, M.E., Ceniceros-Gómez, A.E., Villalobos, M., Romero, F., Santiago, P., 2012. Natural arsenic attenuation via metal arsenate precipitation in soils contaminated with metallurgical wastes: II. Cumulative evidence and identification of minor processes. Appl. Geochem. 27, 2204–2214. http://dx.doi.org/10.1016/j.apgeochem.2012.02.021.
Henderson, P.J., McMartin, I., Hall, G.E., Percival, J.B., Walker, D.A., 1998. The chemical and physical characteristics of heavy metals in humus and till in the vicinity of the base metal smelter at Flin Flon, Manitoba, Canada. Environ. Geol. 34, 39–58.
IUSS Working Group WRB, 2014. World Reference Base for Soil Resources 2014. International Soil Classification System for Naming Soils and Creating Legends for Soil Maps. World Soil Resources Reports No. 106. FAO, Rome.
Jamieson, H.E., 2011. Geochemistry and mineralogy of solid mine waste: essential knowledge for predicting environmental impact. Elements 7, 381–386. http://dx.doi.org/10.2113/gselements.7.6.381.
Knight, R.F., Henderson, P.J., 2006. Smelter dust in humus around Rouyn-Noranda, Quebec. Geochem. Explor. Environ. Anal. 6, 203–214. http://dx.doi.org/10.1144/1467-7873/05-087.
Kříbek, B., Majer, V., Veselovský, F., Nyambe, I., 2010. Discrimination of lithogenic and anthropogenic sources of metals and sulphur in soils of the central-northern part of the Zambian Copperbelt Mining District: a topsoil vs. subsurface soil concept. J. Geochem. Explor. 104, 69–86. http://dx.doi.org/10.1016/j.gexplo.2009.12.005.
Kříbek, B., Majer, V., Knésl, I., Nyambe, I., Mihaljevič, M., Ettler, V., et al., 2014a. Concentrations of arsenic, copper, cobalt, lead and zinc in cassava (*Manihot esculenta* Crantz) growing on uncontaminated and contaminated soils of the Zambian Copperbelt. J. Afr. Earth Sci. 99, 713–723. http://dx.doi.org/10.1016/j.afrearsci.2014.02.009.
Kříbek, B., Majer, V., Pašava, J., Kamona, F., Mapani, B., Keder, J., et al., 2014b. Contamination of soils with dust fallout from the tailings dam at the Rosh Pinah area, Namibia: regional assessment, dust dispersion modeling and environmental consequences. J. Geochem. Explor. 144, 391–408. http://dx.doi.org/10.1016/j.gexplo.2014.01.010.
Kříbek, B., Majer, V., Knésl, I., Keder, J., Mapani, B., Kamona, F., et al., 2016. Contamination of soil and grass in the Tsumeb smelter area, Namibia. Modeling of contaminants dispersion and ground geochemical verification. Appl. Geochem. 64, 75–91. http://dx.doi.org/10.1016/j.apgeochem.2015.07.006.
Lanteigne, S., Schindler, M., McDonald, A.M., Skeries, K., Abdu, Y., Mantha, N.M., et al., 2012. Mineralogy and weathering of smelter-derived spherical particles in soils: implications for the mobility of Ni and Cu in the surficial environment. Water Air Soil Pollut. 223, 3619–3641. http://dx.doi.org/10.1007/s11270-012-1135-3.
Lanteigne, S., Schindler, M., McDonald, A., 2014. Distribution of metals and metalloids in smelter-derived particulate matter in soils and mineralogical insights into their retention and release in a low-T environment. Can. Mineral. 52, 453–471. http://dx.doi.org/10.3749/canmin.52.3.453.
Majzlan, J., Drahota, P., Filippi, M., 2014. Parageneses and crystal chemistry of arsenic minerals. In: Bowell, R.J., Alpers, C.N., Jamieson, H.E., Nordstrom, D.K., Majzlan, J. (Eds.), Arsenic: Environmental Geochemistry, Mineralogy and Microbiology. Reviews in Mineralogy & Geochemistry Vol. 79, pp. 17–184.
Mantha, N.M., Schindler, M., Murayama, M., Hochella Jr., M.F., 2012. Silica- and sulfate-bearing rock coatings in smelter areas: product of chemical weathering and atmospheric pollution I. Formation and mineralogical composition. Geochim. Cosmochim. Acta 85, 254–274. http://dx.doi.org/10.1016/j.gca.2012.01.033.
Mihaljevič, M., Ettler, V., Vaněk, A., Penížek, V., Svoboda, M., Kříbek, B., et al., 2015. Trace elements and the lead isotopic record in marula (*Sclerocarya birrea*) tree rings and soils near the Tsumeb smelter, Namibia. Water Air Soil Pollut. 226, 177. http://dx.doi.org/10.1007/s11270-015-2440-4.
Morales, A., Cruells, M., Roca, A., Bergó, R., 2010. Treatment of copper smelter flue dusts for copper and zinc extraction and arsenic stabilization. Hydrometallurgy 105, 148–154. http://dx.doi.org/10.1016/j.hydromet.2010.09.001.
Pansu, M., Gautheyrou, J., 2006. Handbook of Soil Analysis: Mineralogical, Organic and Inorganic Methods. Springer Verlag, Berlin-Heidelberg.
Podolský, F., Ettler, V., Šebek, O., Ježek, J., Mihaljevič, M., Kříbek, B., et al., 2015. Mercury in soil profiles from metal mining and smelting areas in Namibia and Zambia: distribution and potential sources. J. Soils Sediments 15, 648–658. http://dx.doi.org/10.1007/s11368-014-1035-9.
Quevauviller, P., 1998. Operationally defined extraction procedures for soil and sediment analysis I. Standardization. TrAC Trends Anal. Chem. 17, 289–298. http://dx.doi.org/10.1016/S0165-9936(97)00119-2.
Samuelsson, C., Björkman, B., 1998a. Dust formation mechanism in the gas cleaning system after the copper converting process. I. Sampling and characterisation. Scand. J. Metall. 27, 54–63.
Samuelsson, C., Björkman, B., 1998b. Dust formation mechanism in the gas cleaning system after the copper converting process. II. Thermodynamic studies. Scand. J. Metall. 27, 64–72.
Schindler, M., Mantha, N., Kyser, K.T., Murayama, M., Hochella Jr., M.F., 2012. Shining light on black coatings in smelter-impacted areas. Geosci. Can. 39, 148–157.
Schlesinger, M.E., King, M.J., Sole, K.C., Davenport, W.G., 2011. Extractive Metallurgy of Copper. fifth ed. Elsevier, Oxford.
Shishin, D., Decterov, S.A., 2012. Critical assessment and thermodynamic modeling of the Cu–O and Cu–O–S systems. Calphad 38, 59–70. http://dx.doi.org/10.1016/j.calphad.2012.04.002.
Shishin, D., Hidayat, T., Jak, E., Decterov, S.A., 2013. Critical assessment and thermodynamic modeling of the Cu–Fe–O system. Calphad 41, 160–179. http://dx.doi.org/10.1016/j.calphad.2013.04.001.
Shukurov, N., Kodirov, O., Peitzsch, M., Kersten, M., Pen-Mouratov, S., Steinberger, Y., 2014. Coupling geochemical, mineralogical and microbiological approaches to assess the health of contaminated soil around the Almalyk mining and smelter complex, Uzbekistan. Sci. Total Environ. 476–477, 447–459. http://dx.doi.org/10.1016/j.scitotenv.2014.01.031.
Simonescu, C.M., Teodorescu, V.S., Carp, O., Patron, L., Capatina, C., 2007. Thermal behavior of CuS (covellite) obtained from copper–thiosulfate system. J. Therm. Anal. Calorim. 88, 71–76. http://dx.doi.org/10.1007/s10973-006-8079-z.
Skeaff, J.M., Thibault, Y., Hardy, D.J., 2011. A new method for the characterisation and quantitative speciation of base metal smelter stack particulates. Environ. Monit. Assess. 177, 165–192. http://dx.doi.org/10.1007/s10661-010-1627-9.
Sorooshian, A., Csavina, J., Shingler, T., Dey, S., Brechtel, F.J., Sáez, A.E., et al., 2012. Hygroscopic and chemical properties of aerosols collected near a copper smelter: implications for public and environmental health. Environ. Sci. Technol. 46, 9473–9480. http://dx.doi.org/10.1021/es302275k.
Tesfaye, F., Taskinen, P., 2011. Phase equilibria and thermodynamics of the system Zn–As–Cu–Pb–S at temperatures below 1173 K. Aalto University Publication Series, Science + Technology. Aalto.
Vítková, M., Ettler, V., Johan, Z., Kříbek, B., Šebek, O., Mihaljevič, M., 2010. Primary and secondary phases in copper–cobalt smelting slags from the Copperbelt Province, Zambia. Mineral. Mag. 74, 581–600. http://dx.doi.org/10.1180/minmag.2010.074.4.581.
Vítková, M., Ettler, V., Hyks, J., Astrup, T., Kříbek, B., 2011. Leaching of metals from copper smelter flue dust (Mufulira, Zambian Copperbelt). Appl. Geochem. 26, S263–S266. http://dx.doi.org/10.1016/j.apgeochem.2011.03.120.
Yoder, C.H., Agee, T.M., Ginion, K.E., Hofmann, A.E., Ewanichak, J.E., Schaeffer Jr., C.D., Carroll, M.J., Schaeffer, R.W., McCaffrey, P.M., 2007. The relative stabilities of the copper hydroxyl sulphates. Mineral. Mag. 71, 571–577. http://dx.doi.org/10.1180/minmag.2007.071.5.571.
Yue, Z., Donahoe, R.J., 2009. Experimental simulation of soil contamination by arsenolite. Appl. Geochem. 24, 650–656. http://dx.doi.org/10.1016/j.apgeochem.2008.12.016.